ORIGINAL ARTICLE

JBMR®

HDAC5 Controls MEF2C-Driven Sclerostin Expression in Osteocytes

Marc N Wein,[1] Jordan Spatz,[1,2,3] Shigeki Nishimori,[1] John Doench,[4] David Root,[4] Philip Babij,[5] Kenichi Nagano,[6] Roland Baron,[6] Daniel Brooks,[1,3] Mary Bouxsein,[1,3] Paola Divieti Pajevic,[1] and Henry M Kronenberg[1]

[1]Endocrine Unit, Massachusetts General Hospital, Boston, MA, USA
[2]Harvard–Massachusetts Institute of Technology (MIT) Division of Health Sciences and Technology (HST), Bioastronautics Program, Cambridge, MA, USA
[3]Center for Advanced Orthopaedic Studies, BIDMC, Boston, MA, USA
[4]Broad Institute of MIT and Harvard, Cambridge, MA, USA
[5]Amgen, Inc., Department of Metabolic Disorders, Thousand Oaks, CA, USA
[6]Harvard School of Dental Medicine, Boston, MA, USA

ABSTRACT

Osteocytes secrete paracrine factors that regulate the balance between bone formation and destruction. Among these molecules, sclerostin (encoded by the gene SOST) inhibits osteoblastic bone formation and is an osteoporosis drug target. The molecular mechanisms underlying SOST expression remain largely unexplored. Here, we report that histone deacetylase 5 (HDAC5) negatively regulates sclerostin levels in osteocytes in vitro and in vivo. HDAC5 shRNA increases, whereas HDAC5 overexpression decreases SOST expression in the novel murine Ocy454 osteocytic cell line. HDAC5 knockout mice show increased levels of SOST mRNA, more sclerostin-positive osteocytes, decreased Wnt activity, low trabecular bone density, and reduced bone formation by osteoblasts. In osteocytes, HDAC5 binds and inhibits the function of MEF2C, a crucial transcription factor for SOST expression. Using chromatin immunoprecipitation, we have mapped endogenous MEF2C binding in the SOST gene to a distal intergenic enhancer 45 kB downstream from the transcription start site. HDAC5 deficiency increases SOST enhancer MEF2C chromatin association and H3K27 acetylation and decreases recruitment of corepressors NCoR and HDAC3. HDAC5 associates with and regulates the transcriptional activity of this enhancer, suggesting direct regulation of SOST gene expression by HDAC5 in osteocytes. Finally, increased sclerostin production achieved by HDAC5 shRNA is abrogated by simultaneous knockdown of MEF2C, indicating that MEF2C is a major target of HDAC5 in osteocytes. © 2014 American Society for Bone and Mineral Research.

KEY WORDS: OSTEOCYTES; WNT/ß-CATENIN/LRPS; OSTEOPOROSIS; EPIGENETICS

Introduction

Osteocytes, the most abundant cell type in bone, are important regulators of bone remodeling by producing paracrine factors.[1] Osteocytes express receptor activator of NF-κB ligand (RANKL), a crucial osteoclastogenic cytokine,[2,3] and sclerostin (encoded by SOST), a potent inhibitor of canonical Wnt signaling, which decreases osteoblast number and activity.[4] In humans, lack of SOST owing to loss of function mutations causes high bone mass in the rare disease, sclerosteosis,[5] whereas reduced SOST levels owing to deletion of a downstream intergenic enhancer region causes a milder high bone mass phenotype in Van Buchem disease.[6] Common SOST polymorphisms are associated with bone density and fracture risk variation in the general human population.[7] Sclerostin antibodies are now under investigation for osteoporosis therapy.[8]

Although regulation of SOST expression by parathyroid hormone (PTH)[9–11] and mechanical forces[12–15] has been demonstrated, little is known about molecular mechanisms controlling its expression in osteocytes. The best-studied regulator of SOST expression in osteocytes is the transcription factor MEF2C. Presumably through binding to a downstream enhancer sequence in the intergenic region between SOST and its neighbor MEOX, MEF2C positively regulates SOST expression.[11] Mice lacking MEF2C in osteocytes, or lacking the downstream enhancer region, display reduced SOST levels and high bone mass.[16,17]

Histone deacetylases (HDACs) are a family of enzymes capable of deacetylating lysine residues in a wide variety of cellular

Received in original form June 1, 2014; revised form September 11, 2014; accepted September 25, 2014. Accepted manuscript online September 28, 2014.
Address correspondence to: Henry M Kronenberg, MD, Endocrine Unit, Massachusetts General Hospital, Their 1101, 50 Blossom Street, Boston, MA 02114, USA. E-mail: hkronenberg@mgh.harvard.edu
This article was originally omitted from the issue at first publication. This notice is included in the online and print versions to indicate that both have been corrected February 20, 2015.
This is a Commentary on Mark L Johnson (J Bone Miner Res. 2015;30:397–399. DOI: 10.1002/jbmr.2459)
Additional Supporting Information may be found in the online version of this article.
Journal of Bone and Mineral Research, Vol. 30, No. 3, March 2015, pp 400–411
DOI: 10.1002/jbmr.2381

proteins, including histones.[18] Class IIa HDACs (HDACs 4, 5, 7, and 9) contain N-terminal extensions with phosphoacceptor 14-3-3 binding sites that allow them to sense and transduce signaling information.[19] In addition, the N-termini of class IIa HDACs contain a MEF2-binding site that mediates repression of MEF2-driven gene expression.[20] Although roles for class IIa HDACs in osteoblasts have been described,[21–23] their functions in osteocytes remain largely unexplored. Recently, HDAC5 overexpression was reported to suppress SOST expression in luciferase assays in UMR106 cells.[24] We used loss of function analysis under physiologic conditions to ask whether class IIa HDACs might regulate MEF2C-driven SOST expression in osteocytes. We report that HDAC5 directly controls SOST expression and that mice lacking HDAC5 show increased sclerostin levels in osteocytes, low bone density, and reduced bone formation.

Materials and Methods

Germline HDAC5$^{-/-}$ mice were provided by Dr. Eric Olson and studied at 8 weeks of age. Cell culture experiments were performed using a single-cell subclone of Ocy454 cells (Spatz and colleagues, manuscript in preparation, 2014). Lentiviral infections were performed using protocols available online (www.broadinstitute.org). Sclerostin ELISAs were performed using an antibody pair as described in Yu and colleagues.[25] See Supplemental Information for full details, and see Supplemental Fig. 6 for all PCR primer sequences used.

Results

We sought to establish an in vitro system to dissect mechanisms of SOST expression in osteocytes. Ocy454 cells are a conditionally immortalized cell line with many properties of bone-embedded osteocytes. The line was derived from bitransgenic mice for DMP1-GFP and a thermolabile SV40 large T antigen that is active at 33°C and inactive at 37°C (Spatz and colleagues, manuscript in preparation, 2014). Lentiviral (LV)-based shRNA-mediated gene silencing[26–28] was used to determine the roles of specific genes in regulating SOST expression. Supplemental Fig. S1*A* demonstrates that Ocy454 cells can be infected with a puromycin-resistance-conferring LV expressing a control shRNA (shGFP) and retain sclerostin expression and its regulation by PTH.

We next used shRNA to reduce levels of known SOST-positive and -negative regulators, MEF2C[11,16,17] and Gsα,[29,30] respectively. Gsα shRNA increased SOST expression and sclerostin secretion (Spatz and colleagues, manuscript in preparation, 2014). For MEF2C shRNA, the range of sclerostin expression was determined in each experiment using 8 to 10 control shRNA-expressing lentiviruses targeting nonexpressed genes (LacZ, luciferase, GFP, RFP). Dotted lines indicate two standard deviations above and below the mean value of sclerostin expression in the presence of control shRNAs. LV-mediated shRNA for MEF2C selectively reduced sclerostin secretion (Supplemental Fig. S1*B*; each data point indicates a separate Mef2-targeting hairpin; data for MEF2B is not shown because MEF2B is not expressed in Ocy454 cells), and all the MEF2C-targeting shRNAs effectively reduced MEF2C protein levels (Supplemental Fig. S1*C*).

A similar approach was then used to test the function of class IIa HDACs. As shown in Fig. 1*A*, infection with independent hairpins targeting HDAC5 (but not HDAC4, HDAC7, or HDAC9) increased sclerostin secretion across multiple experiments. For the HDAC5 shRNAs, individual hairpins are labeled next to the corresponding data points in Fig. 1*A*, *B*. The individual hairpins (F9 and F12) that best reduced HDAC5 mRNA and protein levels increased SOST expression (Fig. 1*B* and Supplemental Fig. S1*D*, *E*). In contrast, HDAC4 and HDAC7 shRNAs comparably reduced target mRNA abundance but did not increase SOST (Fig. 1*C*, *D*). HDAC9 is not expressed in Ocy454 cells (data not shown). Although the most effective HDAC4 and HDAC5 shRNAs reduced target mRNA by 60% to 70%, the "best" HDAC5 shRNA (F12) was more effective at reducing target protein levels than the corresponding "best" HDAC4 shRNA (D8) tested (Fig. 1*E*). Although these data support a role for HDAC5 in controlling SOST expression, we cannot rule out a contribution from HDAC4 or HDAC7, given differences in protein knockdown. Because comparable results were found for two independent HDAC5 hairpins (F9 and F12; Fig. 1*B*, Supplemental Fig. S1*D*, and data not shown), the F12 hairpin was used for further study.

Stable HDAC5 (F12) shRNA-expressing Ocy454 subclones were then generated (Fig. 2*A*). These cells display growth kinetics (Fig. 2*B*) comparable to that of control shLacZ-expressing cells. HDAC5 knockdown increases sclerostin secretion, particularly at earlier time points after cells are switched to the nonpermissive growth temperature (Fig. 2*C*). Analysis of a panel of osteocytic genes over the course of differentiation revealed that HDAC5 knockdown targets a subset (SOST and DMP1 but not PHEX) of osteocyte markers (Fig. 2*D*). Osteocytes express the key regulators of osteoclastogenesis, RANKL, and osteoprotegerin (OPG).[2,3,31] HDAC5 shRNA does not affect basal (Supplemental Fig. S2*A*, *B*) or PTH-stimulated (Fig. S2*C*) expression of these factors.

LV overexpression was next used to increase HDAC5 (wild-type (WT) or S259/498A, a constitutively nuclear "super-repressor" version [32] levels in Ocy454 cells (Fig. 2*E*). Although overexpression of either WT or S259/498A HDAC5 does not affect growth kinetics in Ocy454 cells (Fig. 2*F*), overexpression of HDAC5, and especially of the S259/498A nuclear mutant form, reduces SOST expression and sclerostin secretion (Fig. 2*G*, *H*).

To rule out off-target shRNA effects, HDAC5 shRNA cells were rescued with a human HDAC5 cDNA with several synonymous nucleotide changes in the murine shRNA targeting sequences (Fig. 2*I*). As shown in Fig. 2*J*, HDAC5 cDNA rescue reduced sclerostin expression by HDAC5 shRNA cells, providing further evidence that the phenotype owing to HDAC5 (F12) shRNA is because of reduced HDAC5 protein levels.

To show that HDAC5 mRNA is expressed in osteocytes, HDAC5 mRNA levels were analyzed in primary DMP1-GFP^{neg} (osteoblasts and stromal cells) and DMP1-GFP^{pos} (enriched osteocytes) long bone cells isolated from DMP1-GFP mice. As previously reported, the GFP-negative fraction expresses high levels of the osteoblast-specific gene Keratocan,[33,34] whereas SOST mRNA is exclusively detected in the GFP-positive fraction. As shown in Supplemental Fig. S2*D*, HDAC5 mRNA is detected in both fractions, with slightly higher levels present in DMP1-GFP^{pos} cells.

To explore the role of HDAC5 in controlling sclerostin levels in vivo, global HDAC5-knockout (KO) mice were analyzed. These mice are normal appearing and fertile, with reported cardiac and behavioral phenotypes.[35,36] Analysis of calvarial RNA from 8-week-old mice ($n = 12$/group) demonstrates an 84% increase in SOST mRNA levels in the absence of HDAC5 (Fig. 3*A*), with no changes in osteocyte density (Fig. 3*B*). As previously described,[37] sclerostin immunoreactivity is largely confined to deeply embedded osteocytes relatively far from the endocortical surface in WT mouse tibias (Fig. 3*C*, left). In contrast, many more sclerostin-

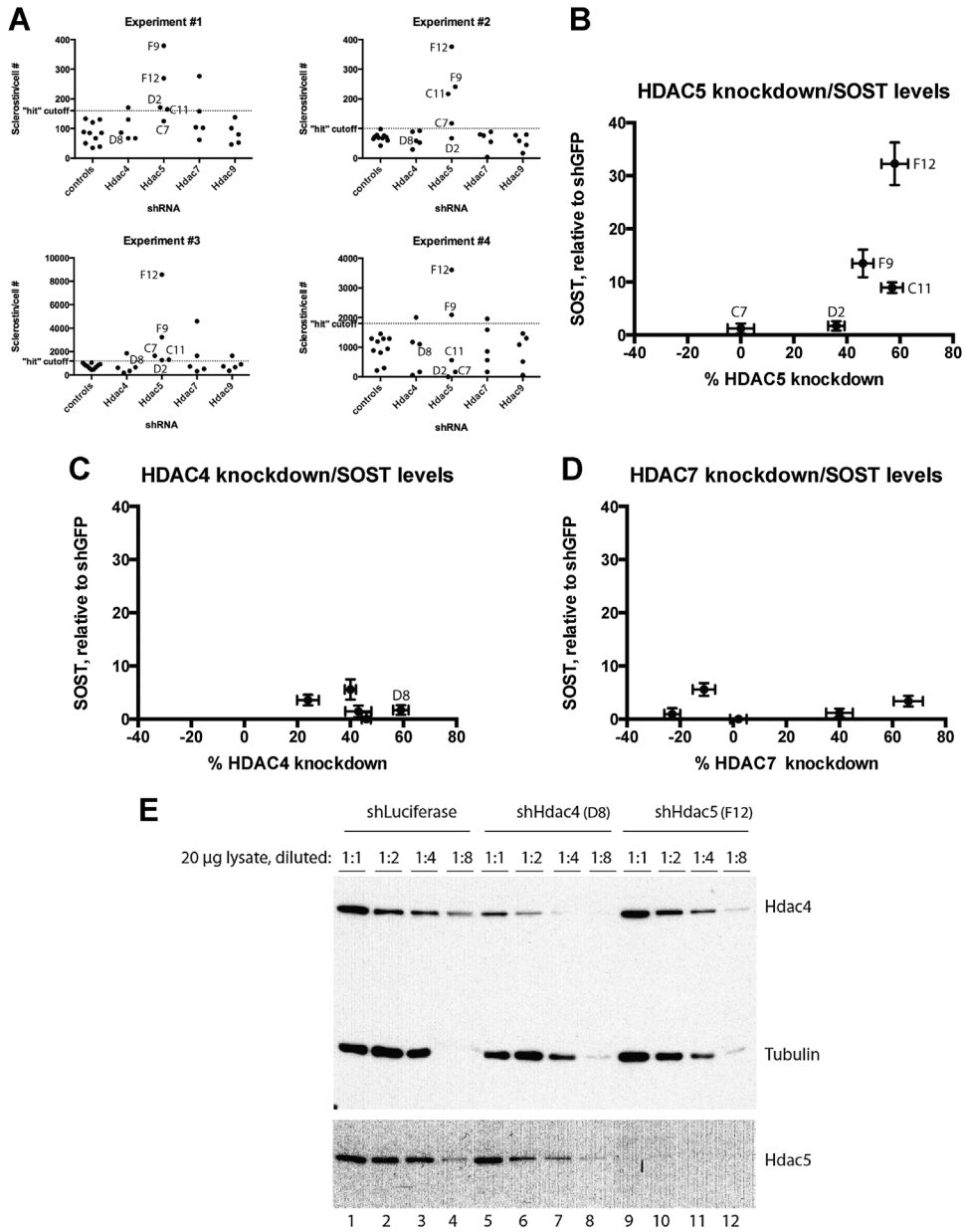

Fig. 1. Identification of HDAC5 as a putative regulator of SOST in vitro. (*A*) Ocy454 cells were infected with 10 separate control shRNA-expressing lentiviruses, and 5 separate shRNAs targeting the indicated class IIa HDAC. Ten days later, sclerostin levels were determined by ELISA and normalized to cell count per well. In experiments 1 and 2, cells were infected after 1 day at 37°C. In experiments 3 and 4, cells were infected after 5 days at 37°C. The "hit" cutoff was determined as 2 standard deviations above the mean control sclerostin levels for each experiment. (*B–D*) Ocy454 cells were infected with individual hairpins targeting the indicated class IIa HDAC or control (shGFP) lentivirus. Ten days later, RNA was prepared and knockdown efficiency and SOST levels were determined for each hairpin (relative to shGFP). (*E*) Protein knockdown for shHDAC4 and shHDAC5 was determined by immunoblotting.

positive osteocytes are close to the endocortical surface in HDAC5-KO sections (Fig. 3*C*, right). The overall percentage of sclerostin-positive osteocytes is modestly increased in the absence of HDAC5 (Fig. 3*D*). In contrast, the percentage of sclerostin-positive peri-endosteal osteocytes (defined as embedded osteocytes within the inner one-quarter of the cortical area) is dramatically increased in HDAC5 knockouts (Fig. 3*E*).

We next investigated the functional consequences of increased osteocytic SOST expression in HDAC5-KO mice. Sclerostin is a Wnt pathway antagonist;[38,39] therefore, we anticipated reduced activity of this pathway in HDAC5-KO mice. Wnt signaling promotes ß-catenin stabilization,[40] in part via inhibiting its N-terminal phosphorylation.[41] Immunostaining for the nonphosphorylated (active) form of ß-catenin revealed reduced staining in endosteal osteoblasts in the absence of HDAC5 (Fig. 4*A*, bottom). Active ß-catenin levels were comparable between genotypes in primary spongiosa cells (Fig. 4*A*, top), suggesting that reduced active ß-catenin in endosteal osteoblasts in the HDAC5-KO strain is a selective phenomenon that correlates with increased sclerostin at this skeletal site. AXIN2, a

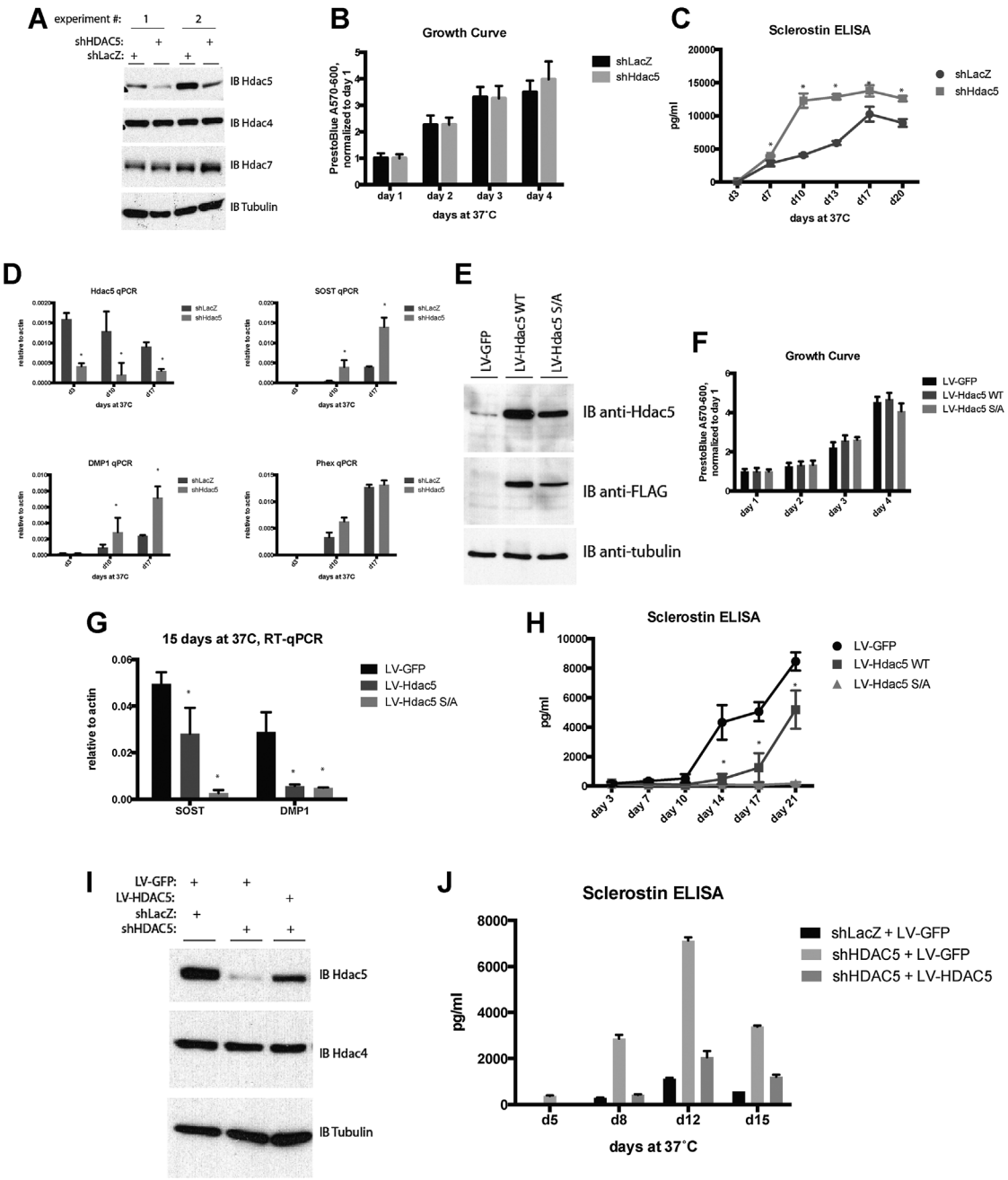

Fig. 2. HDAC5 controls SOST expression in vitro. (*A*) Immunoblot for HDAC5, HDAC4, and HDAC7 from stable shLacZ and shHDAC5-expressing Ocy454 subclones. Tubulin is used as a loading control. (*B*) Growth curve showing comparable expansion kinetics of shLacZ and shHDAC5 cells at 33°C ($n = 42$ wells/cell line). (*C*) Kinetics of sclerostin secretion after identical numbers shLacZ and shHDAC5 cells were switched from 33°C to 37°C for the indicated time. Every 3 to 4 days, conditioned medium was collected and analyzed by sclerostin ELISA ($n = 4$ wells/time point). The p values comparing shLacZ to shHDAC5 are 0.19 at day 3, 0.011 at day 7, 0.00019 at day 10, $1.59^{*}10^{-5}$ at day 14, 0.012 at day 17, and 0.00081 at day 20. (*D*) RNA was isolated from shLacZ and shHDAC5 cells after culture at 37°C for the various times and the levels of the indicated gene were determined by RT-qPCR. All p values for HDAC5 levels comparing control and HDAC5 shRNA are below 0.001. For SOST, at day 3 $p = 0.29$, day 10 $p = 0.043$, day 17 $p = 0.012$. For DMP1, at day 3 $p = 0.84$, day 10 $p = 0.048$, day 17 $p = 0.0041$. (*E*) Immunoblot showing overexpression of FLAG-tagged HDAC5 in Ocy454 cells. (*F*) Growth curve showing comparable expansion kinetics of control and HDAC5-overexpressing cells at 33°C ($n = 12$ wells/cell line). (*G*) Overexpressing cells were analyzed for expression of indicated genes as in (*C*). The p value comparing LV-GFP to LV-HDAC5 WT for SOST is 0.038, and for DMP1 is 0.0091. The p value comparing LV-GFP to LV-HDAC5 S/A for SOST is $9.22^{*}10^{-5}$, and for DMP1 is 0.0081. (*H*) Overexpressing cells were analyzed for sclerostin secretion by ELISA as in (*C*). The p values comparing LV-GFP to LV-HDAC5 WT are 0.023 at day 7, 0.069 at day 10, 0.0056 at day 14, 0.0050 at day 17, and 0.017 at day 20. The p values comparing LV-GFP to LV-HDAC5 S/A cells are 0.0069 at day 7, 0.042 at day 10, 0.0034 at day 14, 0.00018 at day 17, and $2.2^{*}10^{-5}$ at day 21. (*I*) Immunoblot showing HDAC5 and HDAC4 protein levels in HDAC5 shRNA and HDAC5 shRNA plus HDAC5 cDNA cells. (*J*) Sclerostin ELISA from the indicated cells as in (*C*). At all time points, the p value comparing control to shHDAC5 is <0.001, and the p value comparing control to shHDAC5 plus LV-HDAC5 is nonsignificant. For all panels, $^{*}p < 0.05$.

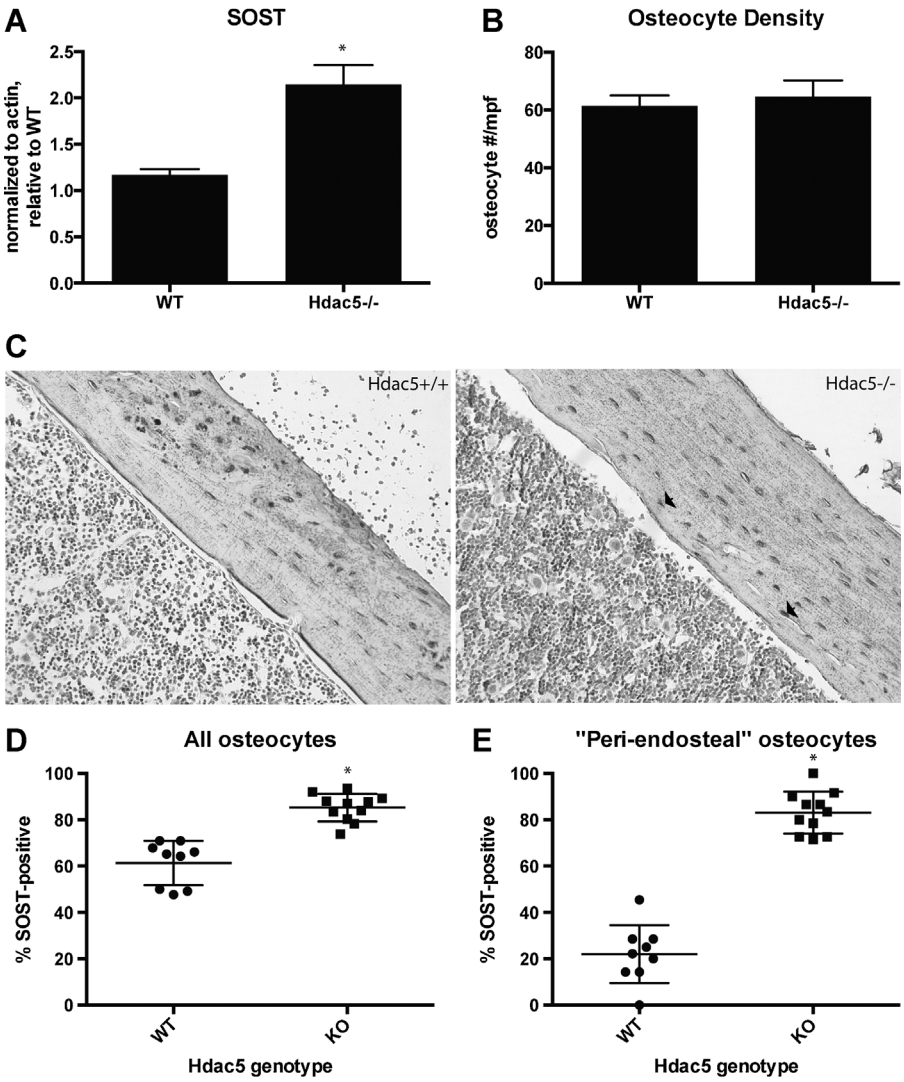

Fig. 3. Increased SOST/sclerostin levels in HDAC5-deficient mice. (*A*) SOST levels relative to ß-actin were determined in calvarial RNA ($n = 12$ samples/genotype) from 8-week-old HDAC5$^{+/+}$ (WT) and HDAC5$^{-/-}$ mice. The p value for the comparison between WT and HDAC5$^{-/-}$ is 0.00019. (*B*) Comparable cortical osteocyte density in WT and HDAC5$^{-/-}$ bone. (*C*) Representative photomicrographs of sclerostin IHC (brown) in cortical bone on the lateral surface of the tibia from WT (right) and HDAC5$^{-/-}$ (left) sections. Arrowheads denote sclerostin-positive osteocytes close to the endosteal surface present in HDAC5$^{-/-}$ tissue. (*D, E*) Quantification of sclerostin immunoreactive cells, $n = 10$ sections from 5 mice scored per genotype. For both comparisons, $p < 0.001$. For all panels, $^{*}p < 0.01$.

canonical Wnt pathway target gene,[42] levels are reduced in HDAC5 KO bone RNA (Fig. 4*B*).

To determine the role of HDAC5 in regulating (directly or indirectly) the expression of molecular markers of differentiation of various bone cell types, control and HDAC5-KO calvarial RNA was profiled for osteoblast (TNALP, BGLAP), osteoclast (ACP5, which encodes Trap5b), osteoclastogenic (TNFSF11 and TNFRSF11B encoding RANKL and OPG), and osteocyte (DMP1, PHEX) marker genes (Fig. 4*C*). No obvious compensation at the mRNA level from the related class IIa HDACs 4 and 7 was observed. Although the expression of the majority of genes were unaffected, two significant differences were found. First, PHEX levels were increased in HDAC5-KO skull RNA. Second, osteocalcin (BGLAP) mRNA levels were decreased. This corresponds to reduced osteocalcin immunostaining in osteoblasts on the endosteal surface in HDAC5-KO mice (Fig. 4*D*). Trabecular bone density in the distal femur of 8-week-old male and female wild-type and HDAC5 KO mice was quantified by μCT. A significant reduction in trabecular bone density was observed in HDAC5 KO mice (Fig. 4*E*, *F* and Supplemental Fig. S3).

To determine the tissue-level consequences of HDAC5 knockout, we performed static and dynamic histomorphometry on tibias of 8-week-old female WT and HDAC5 KO mice. As previously reported,[23] trabecular bone volume (BV/TV) was approximately 40% lower in HDAC5-KO mice (Table 1). This observation was supported by other structural trabecular bone parameters and all parameters showed highly significant differences. In addition, all dynamic parameters of bone formation were significantly reduced in HDAC5-KO mice, with a 40% reduction in mineral apposition rate (MAR) and a 50% reduction

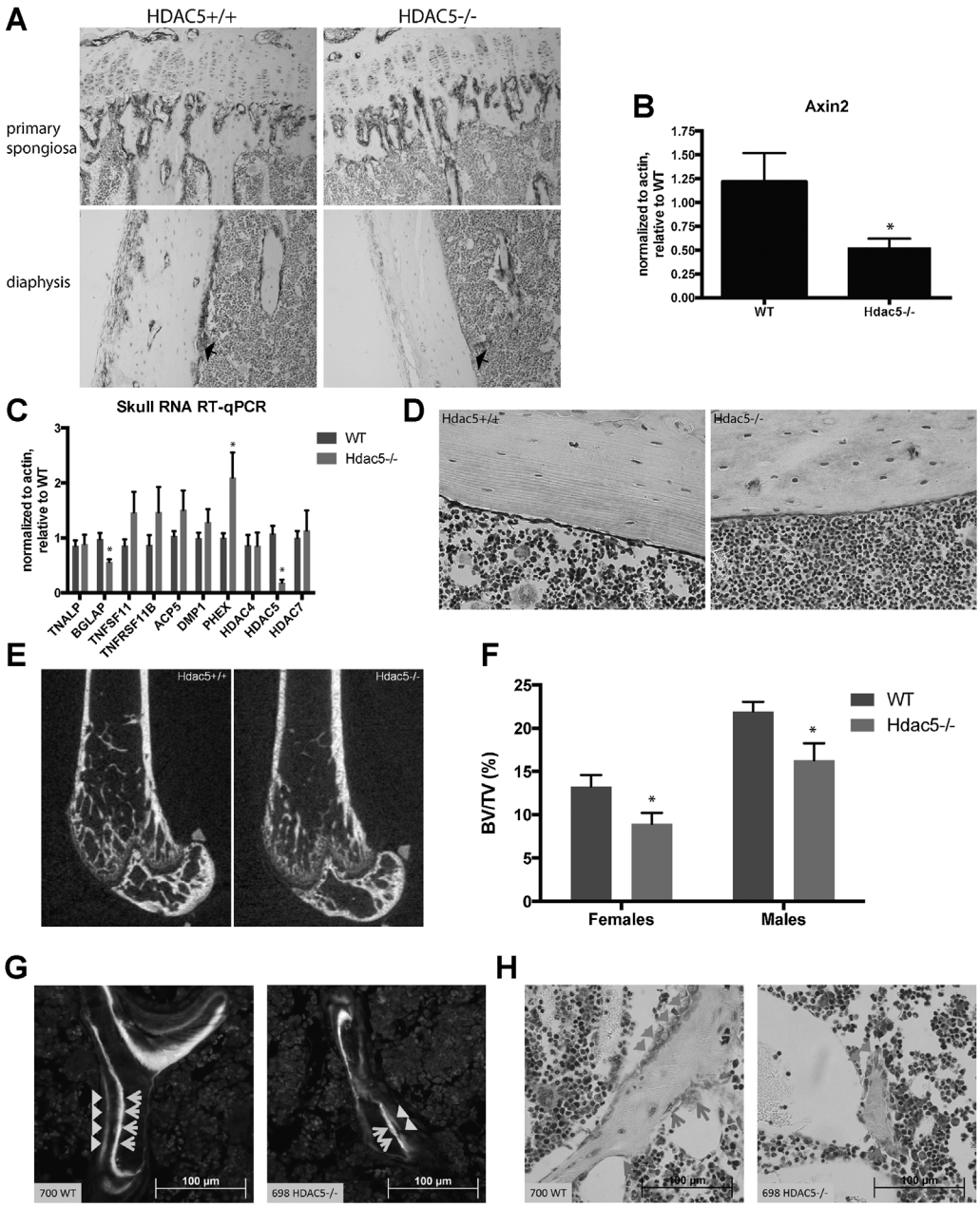

Fig. 4. Skeletal consequences of HDAC5 deficiency. (*A*) Active (non-phospho Ser33/37/Thr41) beta-catenin IHC on tibia sections from WT and HDAC5$^{-/-}$ mice. In the top panel, comparable staining is found in growth plate chondrocytes and cells adjacent to bone surfaces in the primary spongiosa. Reduced staining is observed in cells lining the endosteal surface and in the periosteum (bottom panel, arrowheads), whereas staining intensity is comparable in cells lining trabecular surfaces. (*B*) AXIN2 levels relative to beta-actin were determined in calvarial RNA ($n = 12$ samples/genotype) from 8-week-old mice. The p value comparing AXIN2 levels in WT and HDAC5$^{-/-}$ is <0.0001. (*C*) Levels of the indicated genes relative to beta-actin were determined in calvarial RNA ($n = 12$ samples/genotype) from 8-week-old HDAC5$^{+/+}$ (WT) and HDAC5$^{-/-}$ mice. The p value for BGLAP comparing WT and HDAC5$^{-/-}$ is 0.0022, for PHEX is 0.027, for HDAC5 is less than 0.001. (*D*) Osteocalcin IHC on tibia sections from WT and HDAC5$^{-/-}$ mice. Reduced staining intensity is observed in endosteal osteoblasts in HDAC5$^{-/-}$ tissue. (*E*) Representative µCT sagittal image of the distal femur showing trabecular osteopenia in the absence of HDAC5 in 8-week-old female mice. (*F*) Trabecular bone volume fraction (BV/TV) from the distal femur of 8-week-old female (WT, $n = 11$, HDAC5$^{-/-}$, $n = 10$) and male (WT, $n = 12$, HDAC5$^{-/-}$, $n = 9$). The p value for the comparison between WT and HDAC5$^{-/-}$ females is 0.030, and males is 0.009. Additional µCT parameters are shown in Supplemental Fig. S3. For this figure, $^{*}p < 0.05$. (*G*) Representative fluorescent image showing dual tetracycline labeling component of dynamic histomorphometry. Arrows (light green) show calcein labeling 7 days before death, and arrowheads (light orange) show demeclocycline labeling 2 days before death. (*H*) Representative toluidine blue stain from static histomorphometry. Arrows (red) show TRAP-stained osteoclasts. Arrowheads (orange) show osteoblasts.

Table 1. Histomorphometry Analysis From Proximal Tibia of 8-Week-Old Female Mice

Parameter	WT ($n = 8$)	HDAC5$^{-/-}$ ($n = 9$)	*t*-test *p* Value
BV/TV (%)	6.31 (1.59)	3.68 (1.18)	0.00141**
Tb.Th (μm)	29.8 (2.94)	22.6 (4.13)	0.00091**
Tb.N (/mm)	2.13 (0.45)	1.61 (0.31)	0.0142*
Tb.Sp (μm)	478 (128)	621 (124)	0.0333*
MAR (μm/d)	2.13 (0.24)	1.28 (0.32)	0.00008**
MS/BS (%)	28.7 (3.23)	24.8 (2.85)	0.02812*
BFR/BV (%/yr)	1533 (224.3)	969 (287.8)	0.00106**
BFR/BS ($\mu m^3/\mu m^2$/d)	222 (25.6)	117 (37.8)	0.00003**
Ob.S/B.Pm (%)	15.1 (3.15)	10.4 (2.51)	0.00385**
N.Ob/B.Pm (/mm)	10.3 (2.18)	7.53 (1.69)	0.00940**
OS/BS (%)	7.15 (3.04)	2.8 (1.49)	0.00169**
O.Th (μm)	3.68 (0.33)	2.85 (0.54)	0.00207**
Oc.S/B.Pm (%)	7.63 (1.22)	6.62 (1.77)	0.19850#
N.Oc/B.Pm (/mm)	2.70 (0.37)	2.22 (0.73)	0.11504#
ES/BS (%)	3.05 (1.05)	2.18 (0.94)	0.09356#

Data are expressed as mean (STD).
*$p < 0.05$;
**$p < 0.01$;
#$p =$ n.s.

in bone-formation rate/bone surface (BFR/BS) (Fig. 4*G*), indicating a prominent defect in bone formation. These findings were further confirmed by analysis of cellular parameters, demonstrating reduced osteoblast number and surface per bone perimeter in HDAC5-KO mice. In contrast, osteoclastic parameters (osteoclast number and surface and eroded surface per bone perimeter) were not significantly changed by HDAC5 deficiency (Fig. 4*H*), although there was a trend toward reduced osteoclast parameters. These findings are consistent with our model in which high sclerostin levels in HDAC5-KO mice cause blunted bone formation. Potential causes for the discrepant cellular data presented here and reported by Obri and colleagues[23] are addressed in the Discussion.

Having established that HDAC5 controls sclerostin levels in vitro and in vivo, we focused on the molecular mechanism(s) whereby this occurs. Because class IIa HDACs are known to regulate MEF2 function in many settings,[20] and MEF2C controls SOST expression in vivo[16,17] and in Ocy454 cells (Supplemental Fig. S1*B*), we asked whether HDAC5 could regulate MEF2C function in osteocytes. Endogenous MEF2C and HDAC5 proteins associate in Ocy454 cells (Fig. 5*A*; CREB and Sp1 are used as negative controls). A MEF2-driven reporter[43,44] is more active in HDAC5 shRNA Ocy454 cells than in control LacZ shRNA cells (Fig. 5*B*; MEF2C shRNA serves as a positive control).

Several conserved noncoding sequences downstream of the SOST gene are present[45] in the region deleted in Van Buchem Disease (Fig. 5*C*; each number below the conservation plot corresponds to a different PCR primer set). When a region 45 kB downstream from the SOST transcription start site (termed ECR5[11] by others and SOST'9' here) is deleted in vivo, SOST levels are reduced and high bone mass is observed.[17] Endogenous MEF2C association with the SOST gene has not been reported. We performed chromatin immunoprecipitation (ChIP) to determine MEF2C occupancy in Ocy454 cells cultured at 37°C for 14 days (a time point in which SOST expression is high). MEF2C chromatin association is found in the +45 kB region amplified with primer set 9 (Fig. 5*D*). Histone 3 lysine 27 acetylation (H3K27Ac, a mark of enhancer activity[46]) is also found at this same region (Fig. 5*E*). Because SOST expression is upregulated in Ocy454 cells over time at 37°C (Fig. 2*C*, *H*), we asked whether temporal changes in chromatin dynamics might occur at the +45 kB enhancer. As shown in Fig. 5*F*, SOST upregulation over time is accompanied by increased MEF2C, H3K27Ac, and p300 (another marker of active enhancers[47]) occupancy at this genomic site.

Three lines of evidence support a direct role for HDAC5 in regulating MEF2C activity at the +45 kB SOST enhancer over the course of osteocyte differentiation. First, HDAC5 shRNA causes increased activity of this element, but not of the proximal SOST promoter, in luciferase assays (Supplemental Fig. S4*A*, *B*). MEF2C shRNA reduces the activity of this enhancer (Supplemental Fig. S4*C*). Second, HDAC5 overexpression dose-dependently inhibits the activity of a MEF2-driven reporter from the desmin (Supplemental Fig. S4*D*) and the SOST'9' (+45 kB) enhancer (Supplemental Fig. S4*E*). Third, endogenous HDAC5 association with this region in control (but not HDAC5 shRNA) Ocy454 cells can be detected by ChIP (Fig. 6*A*). In addition to the +45 kB enhancer site, HDAC5 associates with two other putative conserved enhancers with increased H3K27Ac levels. Moreover, HDAC5 +45 kB SOST enhancer occupancy decreases over time at 37°C (Fig. 6*B*), consistent with increased SOST expression. Although HDAC5 itself is a weak deacetylase,[48] it associates with the nuclear corepressor NCoR and the potent class I deacetylase HDAC3.[49,50] Like HDAC5, endogenous NCoR and HDAC3 enhancer occupancy decrease as SOST expression increases (Fig. 6*B*).

We next tested the functional consequences of HDAC5 shRNA on MEF2C binding and the presence of H3K27Ac at the SOST +45 kB enhancer. Increased amounts of MEF2C and H3K27Ac are observed at this site, as well as two other conserved intergenic loci, in HDAC5 shRNA cells (Fig. 6*C* and Supplemental Fig. S5*A*, *B*). HDAC5 S259/498A overexpression reduces region 9 H3K27Ac levels (Fig. 6*D* and Supplemental Fig. S5*C*). Consistent with its proposed role as a sequence-specific scaffolding protein to recruit corepressor complexes to genomic sites,[51] HDAC5 shRNA decreases NCoR and HDAC3 association with the SOST enhancer (Fig. 6*E*).

Finally, we asked whether MEF2C is required for increased SOST production caused by HDAC5 shRNA. Ocy454 cells were infected with shRNA-expressing lentiviruses to knock down HDAC5, MEF2C, or both (Fig. 6*F*). Reducing MEF2C levels in the setting of HDAC5 shRNA decreased sclerostin secretion, indicating that MEF2C is required for the ability of HDAC5 shRNA to increase SOST (Fig. 6*G*, *H*). This confirms our model that HDAC5 knockdown causes a MEF2C gain of function phenotype that drives high sclerostin production.

Discussion

Our data indicate that HDAC5 functions as a negative regulator of MEF2C-dependent SOST expression in osteocytes. This maps (at least in part) to the distal enhancer 45 kB downstream from the SOST transcription start site identified by Leupin, Collette, and Loots and colleagues.[11,17,45] Based on our results, we propose a model (Fig. 7) in which early in osteocyte differentiation, HDAC5 recruits the corepressors NCoR and HDAC3 to the SOST +45 kB enhancer, thus suppressing SOST expression. As osteocyte differentiation occurs, HDAC5 occupancy is reduced, allowing increased binding of MEF2C along with the coactivator p300, which increases H3K27Ac and the ability of this enhancer to

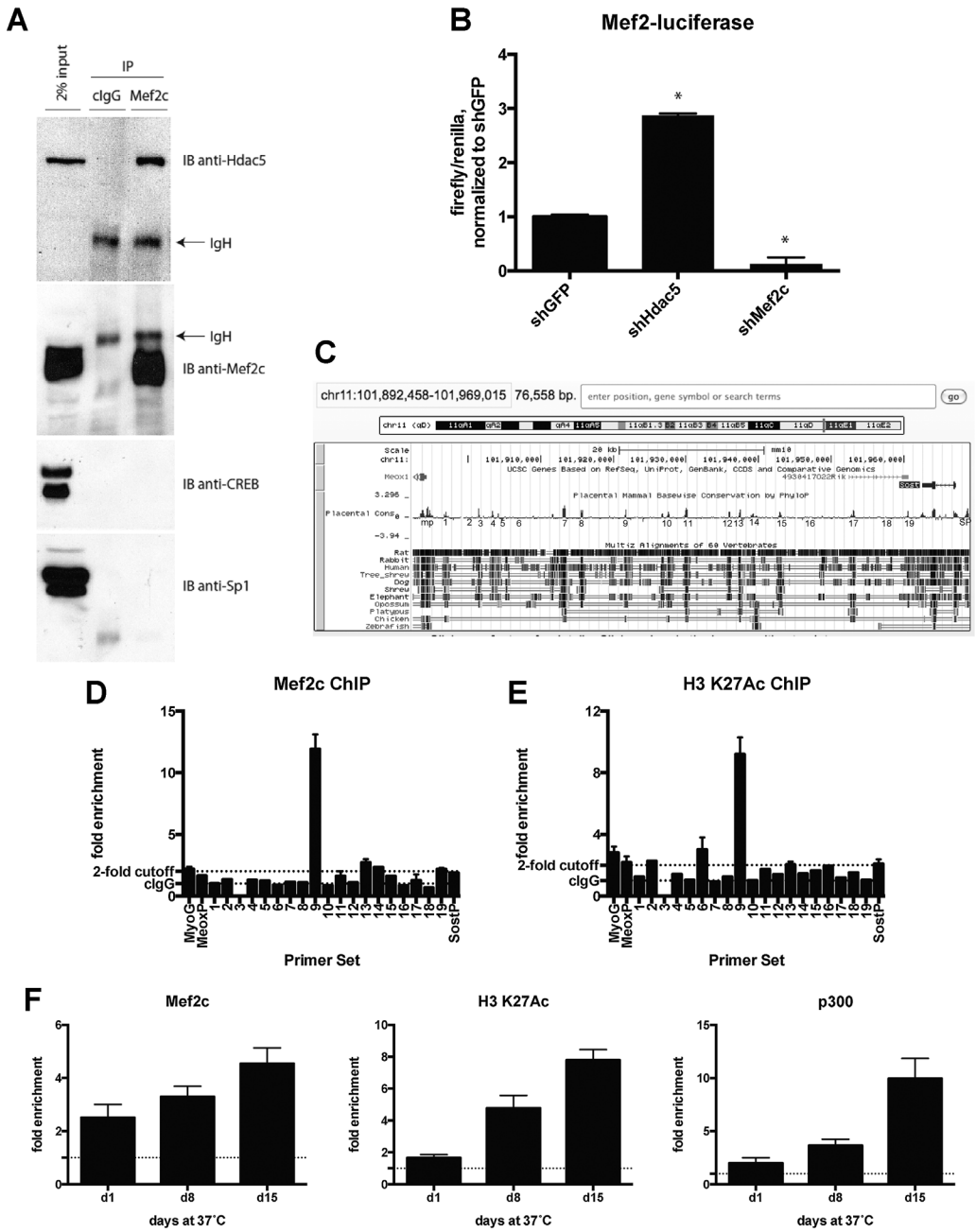

Fig. 5. Increased MEF2C activity in osteocytes lacking HDAC5. (*A*) MEF2C was immunoprecipitated from Ocy454 cells followed by immunoblotting for HDAC5, CREB, and Sp1. (*B*) MEF2-driven luciferase activity relative to renilla was determined in the indicated Ocy454 cells. The *p* values comparing control to HDAC5 shRNA and control to MEF2C shRNA are less than 0.001. (*C*) Interspecies conservation plot from UCSC Genome Browser of mouse chromosome 11 between SOST (right) and MEOX (left). Positions of ChIP PCR primer pairs are shown below. The region corresponding to the human Van Buchem's disease deletion lies approximately between primer sets 3 and 12. (*D, E*) ChIP for MEF2C (*D*) and H3K27Ac (*E*) was performed after culture of Ocy454 cells for 14 days at 37°C. (*F*) ChIP-qPCR using primer set 9 (+45 kB SOST enhancer) for MEF2C, H3K27Ac, and p300 over the course of Ocy454 cell differentiation. For all three antibodies, significantly ($p < 0.01$) increased enrichment was noted at day 15 compared with day 1. For all panels, error bars represent triplicate biological repeats. For all panels, $^{*}p < 0.01$.

promote high levels of SOST expression. Future studies are required to elucidate the signals upstream of HDAC5 during osteocyte differentiation. Additionally, at this point we do not know if HDAC5 functions as a deacetylase or a scaffolding/adaptor protein in osteocytes.

Multiple possible roles for HDAC5 in bone cells have been proposed.[24,52–55] Because HDAC5 is absent in all cells in the HDAC5 knockout mice, we cannot conclude that the skeletal phenotype we observe is solely because of direct actions of HDAC5 in osteocytes. Here, we report that mice lacking HDAC5 in

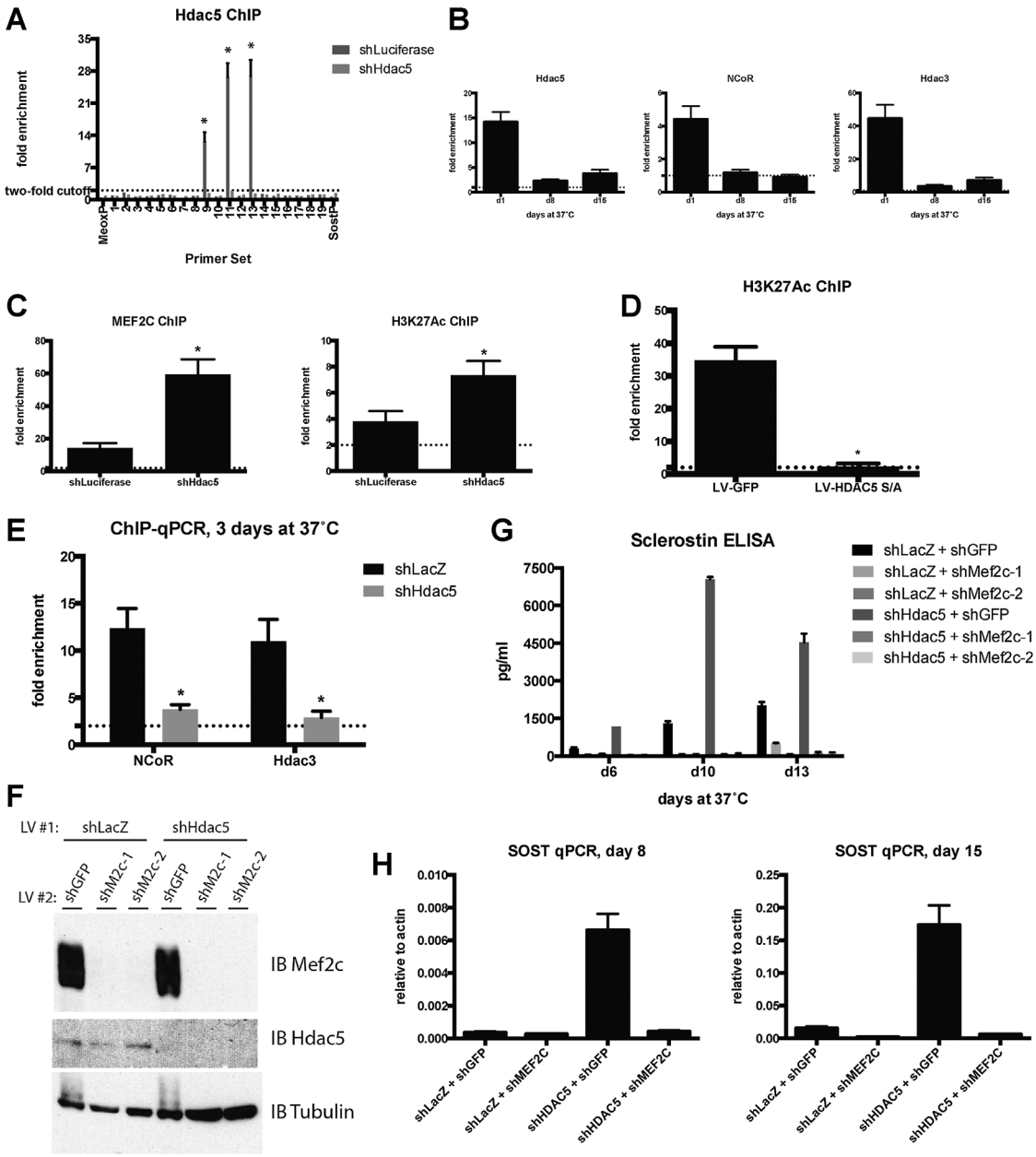

Fig. 6. MEF2C-dependent sclerostin expression is controlled by HDAC5 at the +45 kB SOST enhancer. (*A*) HDAC5 ChIP results from shLacZ or shHDAC5 Ocy454 cells grown at 37°C for 14 days. Error bars represent standard error from biological triplicates; * denotes regions showing HDAC5 association that is reduced with HDAC5 shRNA. (*B*) ChIP-qPCR for HDAC5, NCoR, and HDAC3 was determined over the course of Ocy454 cell differentiation as in Fig. 5*F*. For all three antibodies, significantly ($p < 0.01$) decreased enrichment was noted at day 15 compared with day 1. (*C*) MEF2C and H3K27Ac ChIP comparing control and HDAC5 shRNA Ocy454 cells cultured at 37°C for 14 days; qPCR on recovered DNA was performed using primer set 9. The *p* value comparing shLuciferase and shHDAC5 for Mef2c ChIP is 0.0013, and for H3 K27Ac ChIP is 0.011. (*D*) H3K27Ac ChIP comparing control (LV-GFP) and HDAC5 S259/498A overexpressing cells after 20 days at 37°C, analyzed as in (*C*) except that * indicates decreased H3 K27Ac observed with HDAC5 S259/498A overexpression. The *p* value for primer set 9 comparing shLuc and shHDAC5 for H3 K27Ac ChIP is 0.00018. (*E*) ChIP was performed for NCoR and HDAC3 on control (shLuciferase) and HDAC5 shRNA Ocy454 cells after 3 days in culture at 37°C. qPCR was then performed for the SOST +45 kB enhancer using primer pair 9. The *p* value for NCoR comparing shLuc and shHDAC5 is 0.00231; the *p* value for HDAC3 comparing shLuc and shHDAC5 is 0.00418. (*F*) Immunoblot showing simultaneous knockdown of HDAC5 and MEF2C in Ocy454 cells. (*G*) Sclerostin secretion by the indicated shRNA-expressing cells over time at 37°C. (*H*) SOST RT-qPCR by the indicated shRNA-expressing cells over time at 37°C. Error bars represent values obtained from experimental triplicates. In *G* and *H*, all differences in sclerostin secretion and SOST mRNA levels are statistically significant ($p < 0.001$) comparing control and HDAC5 shRNA and HDAC5 shRNA to HDAC5 shRNA plus MEF2C shRNA. For all panels, * indicates $p < 0.05$ comparing control (shLacZ or LV-GFP) and HDAC5 shRNA or overexpressing cells.

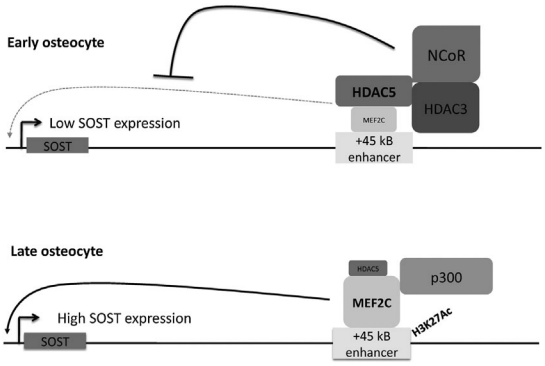

Fig. 7. Schematic representation of the role of HDAC5 in controlling SOST expression in osteocytes. Early in Ocy454 cell differentiation, high levels of HDAC5 are bound to the +45 kB SOST enhancer, thereby blocking MEF2C occupancy and recruiting the corepressors NCoR and HDAC3. Late in Ocy454 cell differentiation, HDAC5 occupancy decreases, thereby permitting increased MEF2C binding, p300 occupancy, and H3 K27 acetylation. See Discussion for further details.

all cells are osteopenic, with high SOST expression and reduced bone formation. In contrast, Obri and colleagues[23] recently reported that HDAC5 functions in osteoblasts to control MEF2C-driven RANKL expression, with increased RANKL in HDAC5-KO mice causing osteopenia owing to high osteoclastic activity. Here, we did not observe a role for HDAC5 in controlling RANKL levels in vitro (Supplemental Fig. S2*A*–*C*) or in vivo (Fig. 4*C*). Furthermore, our histomorphometric analysis (in which TRAP-stained osteoclasts were scored in a blinded manner) revealed normal osteoclast numbers in the HDAC5 knockout mouse (Table 1 and Fig. 4*H*). The same HDAC5-null strain[35] was employed for both the current study and the study of Obri and colleagues. Possibilities to explain these discordant results include differences in genetic background, sex (we analyzed females, whereas Obri and colleagues analyzed males), or skeletal site (we analyzed tibia, whereas Obri and colleagues mainly focused on vertebra). We should note that transgenic mice overexpressing sclerostin in bone are not reported to have increased osteoclastic activity.[45,56] Proof that the osteopenia and reduced osteoblast activity is attributable in part to elevated sclerostin levels will require treatment of HDAC5-deficient mice with, for example, a neutralizing sclerostin antibody.

Sclerostin levels in peri-endosteal osteocytes are increased in the absence of HDAC5 (Fig. 3*C*, *E*), and this correlates with reduced non-phospho beta-catenin staining in nearby endosteal osteoblasts (Fig. 4*A*). However, we observe decreased trabecular bone volume fraction (Fig. 4*E*, *F*) but normal cortical thickness (Supplemental Fig. S3). Quantification of sclerostin levels in cancellous osteocytes is more challenging than in cortical osteocytes, so at this time we cannot correlate this trabecular osteopenia with increased trabecular SOST levels. The absence of a cortical bone phenotype in 8-week-old mice is not entirely unexpected: Transgenic mice overexpressing SOST in bone show trabecular osteopenia but normal cortical thickness.[45,56]

Class IIa HDAC function is controlled by nucleo-cytoplasmic shuttling through dynamic phosphorylation and 14-3-3 binding. In other cell types, N-terminal phosphorylation leads to 14-3-3 association and cytoplasmic retention.[20,44,57] A number of extracellular signals regulate osteocytic SOST expression.[39,58] Recently, it was shown that PTH stimulates HDAC5 dephosphorylation, nuclear translocation, and SOST enhancer binding using overexpression in UMR106 cells.[24] The functional significance of this pathway in osteocytes in vivo remains unknown. Inhibiting HDAC5 N-terminal kinases may be of therapeutic benefit to reduce SOST expression by osteocytes.

The accelerated expression pattern of sclerostin secretion in vitro in HDAC5 shRNA cells (Fig. 2*B*) is consistent with our in vivo immunostaining results (Fig. 3*B*). Sclerostin is considered a marker of "late"/"mature" osteocytes,[59,60] and it is possible that deeply embedded osteocytes are also more "mature" than their peri-endosteal counterparts. An alternative hypothesis is that differential mechanical forces or differences in the extracellular cytokine milieu on peri-endosteal versus deep osteocytes in vivo account for differences in sclerostin expression in these cells. We currently do not know if HDAC5 controls aspects of osteoblast to osteocyte conversion in vivo, as has been demonstrated for Gsα.[29] Although our data suggest a direct role for HDAC5 in regulating SOST expression, we cannot rule out indirect effects on osteocyte biology, illustrated by changes in DMP1 (Fig. 2*C*) or PHEX (Fig. 4*A*) found in its absence.

GWAS data indicate that an intronic HDAC5 SNP (rs228769) is associated with variations in bone mineral density (BMD).[61] Single-nucleotide polymorphisms (SNPs) in MEF2C and SOST also control BMD,[61,62] suggesting the importance of the MEF2C/HDAC5/SOST pathway in humans. A cluster of BMD-regulating SNPs in SOST maps to the human orthologous region to the mouse +45 kB enhancer.[63] The effects of these sequence variants on MEF2C or HDAC5 binding remains unexplored. In conclusion, here we show that HDAC5, a gene associated with BMD variation in humans, is a direct negative regulator of MEF2C-driven sclerostin expression in osteocytes, both in vitro and in vivo.

Disclosures

Philip Babij is an employee of Amgen, Inc. and has received stock and stock options from Amgen, Inc. All other authors state that they have no conflicts of interest.

Acknowledgments

This work was supported by the NIH grants 5T32DK007028 and 1F32DK100215-01 (MW), P01DK11794 (HK), 5UH3AR059655-04 (PDP), and the Ellison Foundation (HK). JMS was supported by Northrop Grumman, MIT Hugh Hampton Young Fellowship, and the NSBRI NASA NCC 9-58.

We thank Forest Lai and Elizabeth Williams for technical support, Dr. Eric Olson for providing mice, Dr. Thomas Lisse for advice with ChIP, Dr. Keertik Fulzele for assistance with osteocalcin IHC, and Dorothy Hu for histology expertise. We thank Dr. Tatsuya Kobayashi and Dr. Keertik Fulzele for comments on this article.

Authors' roles: MNW designed and performed the experiments, analyzed data, and wrote the manuscript. JS, SN, JD, PB, DR, and PDP contributed reagents, designed experiments, and edited the manuscript. KN and RB performed and analyzed histomorphometry measurements and edited the manuscript. DB and MB performed and analyzed μCT measurements and edited the manuscript. HMK designed experiments, analyzed data, and wrote and edited the manuscript.

References

1. Bonewald LF. The amazing osteocyte. J Bone Miner Res. 2011 Feb;26(2):229–38.
2. Nakashima T, Hayashi M, Fukunaga T, et al. Evidence for osteocyte regulation of bone homeostasis through RANKL expression. Nat Med. 2011;17(10):1231–4.
3. Xiong J, Onal M, Jilka RL, Weinstein RS, Manolagas SC, O'Brien CA. Matrix-embedded cells control osteoclast formation. Nat Med. 2011;17(10):1235–41.
4. Li X, Ominsky MS, Niu QT, et al. Targeted deletion of the sclerostin gene in mice results in increased bone formation and bone strength. J Bone Miner Res. 2008 Jun;23(6):860–9.
5. Brunkow ME, Gardner JC, Van Ness J, et al. Bone dysplasia sclerosteosis results from loss of the SOST gene product, a novel cystine knot-containing protein. Am J Hum Genet. 2001 Mar;68(3): 577–89.
6. Balemans W, Patel N, Ebeling M, et al. Identification of a 52 kb deletion downstream of the SOST gene in patients with van Buchem disease. J Med Genet. 2002 Feb;39(2):91–7.
7. Richards JB, Zheng HF, Spector TD. Genetics of osteoporosis from genome-wide association studies: advances and challenges. Nat Rev Genet. 2012 Aug;13(8):576–88.
8. McClung MR, Grauer A, Boonen S, et al. Romosozumab in postmenopausal women with low bone mineral density. N Engl J Med. 2014 Jan 30;370(5):412–20.
9. Keller H, Kneissel M. SOST is a target gene for PTH in bone. Bone. 2005 Aug;37(2):148–58.
10. Bellido T, Ali AA, Gubrij I, et al. Chronic elevation of parathyroid hormone in mice reduces expression of sclerostin by osteocytes: a novel mechanism for hormonal control of osteoblastogenesis. Endocrinology. 2005 Nov;146(11):4577–83.
11. Leupin O, Kramer I, Collette NM, et al. Control of the SOST bone enhancer by PTH using MEF2 transcription factors. J Bone Miner Res. 2007 Dec;22(12):1957–67.
12. Lin C, Jiang X, Dai Z, et al. Sclerostin mediates bone response to mechanical unloading through antagonizing Wnt/beta-catenin signaling. J Bone Miner Res. 2009 Oct;24(10):1651–61.
13. Tu X, Rhee Y, Condon KW, et al. Sost downregulation and local Wnt signaling are required for the osteogenic response to mechanical loading. Bone. 2012 Jan;50(1):209–17.
14. Robling AG, Niziolek PJ, Baldridge LA, et al. Mechanical stimulation of bone in vivo reduces osteocyte expression of Sost/sclerostin. J Biol Chem. 2008 Feb 29;283(9):5866–75.
15. Spatz JM, Ellman R, Cloutier AM, et al. Sclerostin antibody inhibits skeletal deterioration due to reduced mechanical loading. J Bone Miner Res. 2012 Apr;28(4):865–74.
16. Kramer I, Baertschi S, Halleux C, Keller H, Kneissel M. Mef2c deletion in osteocytes results in increased bone mass. J Bone Miner Res. 2012 Feb;27(2):360–73.
17. Collette NM, Genetos DC, Economides AN, et al. Targeted deletion of Sost distal enhancer increases bone formation,bone mass. Proc Natl Acad Sci USA. 2012 Aug 28;109(35):14092–7.
18. Choudhary C, Kumar C, Gnad F, et al. Lysine acetylation targets protein complexes and co-regulates major cellular functions. Science. 2009 Aug 14;325(5942):834–40.
19. Martin M, Kettmann R, Dequiedt F. Class IIa histone deacetylases: regulating the regulators. Oncogene. 2007 Aug 13;26(37):5450–67.
20. Haberland M, Montgomery RL, Olson EN. The many roles of histone deacetylases in development and physiology: implications for disease and therapy. Nat Rev Genet. 2009 Jan;10(1):32–42.
21. Shimizu E, Selvamurugan N, Westendorf JJ, Olson EN, Partridge NC. HDAC4 represses matrix metalloproteinase-13 transcription in osteoblastic cells, and parathyroid hormone controls this repression. J Biol Chem. 2010 Mar 26;285(13):9616–26.
22. Shimizu E, Nakatani T, He Z, Partridge NC. Parathyroid hormone regulates histone deacetylase (HDAC) 4 through protein kinase A-mediated phosphorylation and dephosphorylation in osteoblastic cells. J Biol Chem. 2014 Aug 1;289(31):21340–50.
23. Obri A, Makinistoglu MP, Zhang H, Karsenty G. HDAC4 integrates PTH and sympathetic signaling in osteoblasts. J Cell Biol. 2014 Jun 23;205(6):771–80.
24. Baertschi S, Baur N, Lueders-Lefevre V, Voshol J, Keller H. Class I and IIa histone deacetylases have opposite effects on sclerostin gene regulation. J Biol Chem. 2014 Sep 5;289(36):24995–5009.
25. Yu L, van der Valk M, Cao J, et al. Sclerostin expression is induced by BMPs in human Saos-2 osteosarcoma cells but not via direct effects on the sclerostin gene promoter or ECR5 element. Bone. 2011 Dec;49(6):1131–40.
26. Root DE, Hacohen N, Hahn WC, Lander ES, Sabatini DM. Genome-scale loss-of-function screening with a lentiviral RNAi library. Nat Methods. 2006 Sep;3(9):715–9.
27. Moffat J, Grueneberg DA, Yang X, et al. A lentiviral RNAi library for human and mouse genes applied to an arrayed viral high-content screen. Cell. 2006 Mar 24;124(6):1283–98.
28. Wein MN, Jones DC, Glimcher LH. Lentivirus delivery of shRNA constructs into osteoblasts. Methods Mol Biol. 2008;455:149–55.
29. Wu JY, Aarnisalo P, Bastepe M, et al. Gsalpha enhances commitment of mesenchymal progenitors to the osteoblast lineage but restrains osteoblast differentiation in mice. J Clin Invest. 2011 Sep;121(9): 3492–504.
30. Fulzele K, Krause DS, Panaroni C, et al. Myelopoiesis is regulated by osteocytes through Gsalpha-dependent signaling. Blood. 2013 Feb 7;121(6):930–9.
31. Wijenayaka AR, Kogawa M, Lim HP, Bonewald LF, Findlay DM, Atkins GJ. Sclerostin stimulates osteocyte support of osteoclast activity by a RANKL-dependent pathway. PLoS One. 2011;6(10):e25900.
32. Vega RB, Harrison BC, Meadows E, et al. Protein kinases C and D mediate agonist-dependent cardiac hypertrophy through nuclear export of histone deacetylase 5. Mol Cell Biol. 2004 Oct;24(19): 8374–5.
33. Igwe JC, Gao Q, Kizivat T, Kao WW, Kalajzic I. Keratocan is expressed by osteoblasts and can modulate osteogenic differentiation. Connect Tissue Res. 2011 Oct;52(5):401–7.
34. Paic F, Igwe JC, Nori R, et al. Identification of differentially expressed genes between osteoblasts and osteocytes. Bone. 2009 Oct;45(4): 682–92.
35. Chang S, McKinsey TA, Zhang CL, Richardson JA, Hill JA, Olson EN. Histone deacetylases 5 and 9 govern responsiveness of the heart to a subset of stress signals and play redundant roles in heart development. Mol Cell Biol. 2004 Oct;24(19):8467–76.
36. Renthal W, Maze I, Krishnan V, et al. Histone deacetylase 5 epigenetically controls behavioral adaptations to chronic emotional stimuli. Neuron. 2007 Nov 8;56(3):517–29.
37. Hasegawa T, Amizuka N, Yamada T, et al. Sclerostin is differently immunolocalized in metaphyseal trabecules and cortical bones of mouse tibiae. Biomed Res. 2013 Jun;34(3):153–9.
38. Baron R, Kneissel M. WNT signaling in bone homeostasis and disease: from human mutations to treatments. Nat Med. 2013 Feb;19(2):179–92.
39. Williams BO, Insogna KL. Where Wnts went: the exploding field of Lrp5 and Lrp6 signaling in bone. J Bone Miner Res. 2009 Feb;24(2): 171–8.
40. Hernandez AR, Klein AM, Kirschner MW. Kinetic responses of beta-catenin specify the sites of Wnt control. Science. 2012 Dec 7;338(6112):1337–40.
41. Liu C, Li Y, Semenov M, et al. Control of beta-catenin phosphorylation/degradation by a dual-kinase mechanism. Cell. 2002 Mar 22;108(6):837–47.
42. van Amerongen R, Bowman AN, Nusse R. Developmental stage and time dictate the fate of Wnt/beta-catenin-responsive stem cells in the mammary gland. Cell Stem Cell. 2012 Sep 7;11(3):387–400.
43. Naya FJ, Wu C, Richardson JA, Overbeek P, Olson EN. Transcriptional activity of MEF2 during mouse embryogenesis monitored with a MEF2-dependent transgene. Development. 1999 May;126(10):2045–52.
44. Kozhemyakina E, Cohen T, Yao TP, Lassar AB. Parathyroid hormone-related peptide represses chondrocyte hypertrophy through a protein phosphatase 2A/histone deacetylase 4/MEF2 pathway. Mol Cell Biol. 2009 Nov;29(21):5751–62.

45. Loots GG, Kneissel M, Keller H, et al. Genomic deletion of a long-range bone enhancer misregulates sclerostin in Van Buchem disease. Genome Res. 2005 Jul;15(7):928–35.
46. Zhou VW, Goren A, Bernstein BE. Charting histone modifications and the functional organization of mammalian genomes. Nat Rev Genet. 2010 Jan;12(1):7–18.
47. Visel A, Blow MJ, Li Z, et al. ChIP-seq accurately predicts tissue-specific activity of enhancers. Nature. 2009 Feb 12;457(7231):854–8.
48. Lahm A, Paolini C, Pallaoro M, et al. Unraveling the hidden catalytic activity of vertebrate class IIa histone deacetylases. Proc Natl Acad Sci USA. 2007 Oct 30;104(44):17335–40.
49. Fischle W, Dequiedt F, Hendzel MJ, et al. Enzymatic activity associated with class II HDACs is dependent on a multiprotein complex containing HDAC3 and SMRT/N-CoR. Mol Cell. 2002 Jan;9(1):45–57.
50. Greco TM, Yu F, Guise AJ, Cristea IM. Nuclear import of histone deacetylase 5 by requisite nuclear localization signal phosphorylation. Mol Cell Proteomics. 2011 Feb;10(2):M110.004317.
51. Lobera M, Madauss KP, Pohlhaus DT, et al. Selective class IIa histone deacetylase inhibition via a nonchelating zinc-binding group. Nat Chem Biol. 2013 May;9(5):319–25.
52. Jeon EJ, Lee KY, Choi NS, et al. Bone morphogenetic protein-2 stimulates Runx2 acetylation. J Biol Chem. 2006 Jun 16;281(24): 16502–11.
53. Kang JS, Alliston T, Delston R, Derynck R. Repression of Runx2 function by TGF-beta through recruitment of class II histone deacetylases by Smad3. Embo J. 2005 Jul 20;24(14):2543–55.
54. Li H, Xie H, Liu W, et al. A novel microRNA targeting HDAC5 regulates osteoblast differentiation in mice and contributes to primary osteoporosis in humans. J Clin Invest. 2009 Dec;119(12):3666–77.
55. Kim JH, Kim K, Youn BU, et al. RANKL induces NFATc1 acetylation, stability via histone acetyltransferases during osteoclast differentiation. Biochem J. 2011 Jun 1;436(2):253–62.
56. Rhee Y, Allen MR, Condon K, et al. PTH receptor signaling in osteocytes governs periosteal bone formation and intracortical remodeling. J Bone Miner Res. 2011 May;26(5):1035–46.
57. Parra M, Verdin E. Regulatory signal transduction pathways for class IIa histone deacetylases. Curr Opin Pharmacol. 2010 Aug;10(4):454–60.
58. Galea GL, Meakin LB, Sugiyama T, et al. Estrogen receptor alpha mediates proliferation of osteoblastic cells stimulated by estrogen and mechanical strain, but their acute down-regulation of the Wnt antagonist Sost is mediated by estrogen receptor beta. J Biol Chem. 2013 Mar 29;288(13):9035–48.
59. Rosser J, Bonewald LF. Studying osteocyte function using the cell lines MLO-Y4 and MLO-A5. Methods Mol Biol. 2012;816:67–81.
60. Woo SM, Rosser J, Dusevich V, Kalajzic I, Bonewald LF. Cell line IDG-SW3 replicates osteoblast-to-late-osteocyte differentiation in vitro and accelerates bone formation in vivo. J Bone Miner Res. 2011 Nov;26(11):2634–46.
61. Rivadeneira F, Styrkarsdottir U, Estrada K, et al. Twenty bone-mineral-density loci identified by large-scale meta-analysis of genome-wide association studies. Nat Genet. 2009 Nov;41(11):1199–206.
62. Estrada K, Styrkarsdottir U, Evangelou E, et al. Genome-wide meta-analysis identifies 56 bone mineral density loci and reveals 14 loci associated with risk of fracture. Nat Genet. 2012 May;44(5):491–501.
63. Styrkarsdottir U, Halldorsson BV, Gretarsdottir S, et al. New sequence variants associated with bone mineral density. Nat Genet. 2009 Jan;41(1):15–7.